

# Automatic Working Area Classification in Peripheral Blood Smears Using Spatial Distribution Features Across Scales

W. Xiong<sup>1</sup>, S.H. Ong<sup>2</sup>, J.H. Lim<sup>1</sup>, N.N. Tung<sup>3</sup>, J. Liu<sup>1</sup>,  
D. Racoceanu<sup>4</sup>, K. Tan<sup>5</sup>, A. Chong<sup>5</sup>, K. Foong<sup>6</sup>

<sup>1</sup>Institute for Infocomm Research, A-STAR, Singapore; <sup>2</sup>Department of ECE, National University of Singapore; <sup>3</sup>Vietnam National University –Ho Chi Minh City; <sup>4</sup>French National Research Center (CNRS) and IPAL; <sup>5</sup>Department of Microbiology, the National University of Singapore; <sup>6</sup>Faculty of Dentistry, the National University of Singapore

<sup>1</sup>{wxiong, joohtwee, jliu}@I2R.a-star.edu.sg; <sup>2</sup>eleshong@nus.edu.sg; <sup>3</sup>stuntn@i2r.a-star.edu.sg; <sup>4</sup>daniel@comp.nus.edu.sg; <sup>5</sup>mictank@nus.edu.sg; <sup>6</sup>kelvinfoong@nus.edu.sg

## Abstract

Automatic classification of working areas in peripheral blood smears can provide objective and reproducible quality control for the evaluation of smears and smear maker devices. However, it has drawn little research attention. In this paper we study this topic using image analysis and statistical pattern recognition methods. We employ generic features without requiring the extraction of individual cells. Two new spatial distribution features across scales are defined and utilized to classify working areas. We demonstrate that the only feature and method proposed in a similar work by others is insufficient to characterize the goodness of working areas, particularly the cell distribution. However, by utilizing it together with the features developed in this paper, we can achieve much better results. Our method has been tested on about 150 labeled images acquired from three malaria-infected Giemsa-stained blood smears using an oil immersion 100x objective lens.

## 1. Introduction

Peripheral blood smears are widely used in biological and pathological applications. They are usually prepared using the wedge technique [1] where a wedge is pulled to spread a drop of blood sample on a glass slide. This produces a gradual decrease in thickness of the blood from thick to thin ends with the smear terminating in a feathered edge [1]. In the thick

end, most of the cells are clumped, which increases the difficulty in identifying and analyzing blood components. The central portion of the slide has definite margins on all sides that are accessible to examination by oil immersion objective lenses. Within the thin section towards the feathered end, erythrocytes are distributed in a monolayer. This is the inspection area to acquire images for enumeration, diagnosis, storing, transmitting and processing. The thin end of the film becomes thinner gradually and finally the cells distribute unevenly and may have grainy streaks, troughs, ridges, waves or holes, resulting in insufficient useful information. Correspondingly, there are three typical types of areas in terms of cell separated: clumped, good and sparse, as shown in Fig.1.

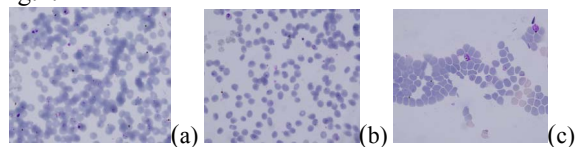


**Figure 1. Typical cell-separation images: (a) clumped, (b) good, and (c) sparse**

The quality of smears and their local areas vary with many factors. The thickness of the spread is influenced by the preparation procedure. The appearances of the image (and the cell) are affected by the concentration of stains, anti-coagulants, lighting, and so on. For example, there will ideally be pale-staining central zones (PCZ) in cells from the Giemsa-stained smears caused by their biconcavity [2]. However, PCZs may

appear rather unclear and not observable.

We use the term *good working areas* (GWAs) to refer to those areas within the thin sections having enough but well-separated representative components (such as cells) with acceptable morphology [3][4]. Because of the variability of wedge smears in their morphology and quality, the range of GWAs on different slides is variable and there are often difficult decisions, even for a well-trained professional, to be made at the time of smear inspection as to where to start the examination [5]. Furthermore, such a manual procedure is inconsistent, prone to error and tedious as ideally one should examine as many as possible such areas to avoid statistical bias.

It is thus desirable to develop automatic GWA detection methods and this becomes necessary for data processing and telepathology applications [4]. Such a task is however challenging as it involves image understanding and characterization in terms of its quality and spatial distribution of feature. Providing *robust solutions* to these tasks and adapting to the *variety* of GWAs due to so many different influences is also not simple. We can only find two relevant publications in the public domain [4][5]. Reference [5] uses the ratio of the total object area over the total object perimeters, called the area-perimeter ratio ( $\eta$ ). This feature alone cannot capture the *goodness* of GWAs in both distribution and morphology as demonstrated later. Reference [4] defines two ratios of numbers of cells, cell centers and cells with centers based on the extraction of the PCZ, which is not always clearly observable.

In this work, we introduce generic features to quantify the goodness of GWAs without requiring the extraction of individual cells. We measure the cell distribution by using spatial occupancy. Across scales, we define two metrics for feature homogeneity. Finally a multi-class support vector machine (SVM) is applied to classify these areas. We validate our method using images acquired from malaria-infected Giemsa-stained blood smears using a digital imaging system under an oil immersion 100x objective lens.

## 2. Quantification of working area goodness

Methods in literature discussing the spatial distribution of features consist of two categories depending on whether individual feature measuring is required [6] or not [7]. As we do not extract individual cells, we study the latter [7]. The spatial occupancy  $\alpha$  of a feature  $E$  in  $\Omega$  is defined as

$$\alpha = \frac{\iint_{\Omega} f(x, y) dx dy}{\iint_{\Omega} dx dy}, \quad (1)$$

Here  $f(x, y)$  is 1 if  $(x, y)$  belongs to  $E$  and 0 otherwise. We consider a pyramid image representation. We partition  $f(x, y)$  in the two dimensions into equal blocks and represent it in a pyramid with four quadrants  $Q(k, n)$  at each hierarchical level  $k$ ,  $k=0, \dots, K$ , and each node  $n, n=1, \dots, 4$ , from coarse scales ( $k=0$ , without partitioning) to fine ( $k=K$ ). Each parent node  $Q(k, n)$  has four child quadrants. Hence, at each level  $k$ , there are  $2^k$  rows and  $2^k$  columns of blocks  $B_k(i, j)$ ,  $i=1, \dots, 2^k$ ,  $j=1, \dots, 2^k$ . Denoting the occupancy in  $B_k(i, j)$  by  $\alpha_k(i, j)$ , the mean and the standard derivation are, respectively,

$$\mu_k = \sum_{i=1}^{2^k} \sum_{j=1}^{2^k} \alpha_k(i, j) / 4^k, k=0, \dots, K, \quad (2)$$

$$\sigma_k = \sqrt{\sum_{i=1}^{2^k} \sum_{j=1}^{2^k} (\alpha_k(i, j) - \mu_k)^2 / (4^k - 1)}, k=1, \dots, K. \quad (3)$$

Reference [7] relates the fat distribution to the levels of the pyramid representation and finds that low values of standard deviation at low levels mean a uniform distribution, while high values mean a nonuniform distribution. In order to take advantage of all scales of information, we further define the spatial homogeneity of  $f(x, y)$  as the mean of the variance

across scales:  $\lambda = \sum_{k=1}^K \sigma_k^2 / K$ . Fig. 2 shows a curve of

$\sigma_k$  versus level index  $k$  for the three typical images shown in Fig. 1. We observe that the “good” image has a lower value of area under its curve. Hence, we

include the area  $\tau = \sum_{k=1}^K \sigma_k$  as a new feature. The

above features encode the object sizes and spatial organizations. To characterize the degree of cell clumping, we adopt  $\eta$  [5], which measures overlap implicitly as clumped cells have a larger dimension.

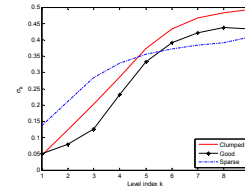


**Figure 2 Standard derivations of occupancy versus pyramid levels**

### 3. Methodology

Our method comprises four steps: 1) image preprocessing, 2) connected component labeling and feature extraction, 3) model parameters learning; and 4) working area classification.

During image analysis, a captured image is first converted to the hue-saturation-value color space. Its luminance value channel is then chosen for further processing. In the original images, the cells appear dimmer than the background (see Fig. 1). The complement of this luminance channel is obtained to make the cells look brighter than the background (shown in Fig. 3(a)). Images in this channel are basically bimodal (see Fig. 3(b)). The brighter mode (the foreground) consists of RBCs whose morphology and distribution are our prime concerns. We apply morphological operations to remove noise.

Otsu's binarization method [8] chooses the threshold to minimize the intra-class variance of the black and white pixels. It is a simple method to produce binary images (Fig. 3(c)) and robust to different illumination and color changes. We analyze this binary image to find white connected components, called objects. Each object may contain multiple cells. In this work, we make no attempt to separate individual cells from objects, which is still very challenging in general. Each object is then labeled as shown in Fig. 3(d) by squares. For each object, we compute its area, perimeter, and the equivalent diameter.

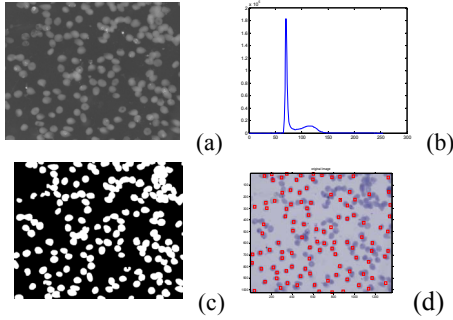


**Figure 3. (a) Gray level images, (b) its histogram, (c) the binary image, and (d) the labeled objects.**

We employ SVM for the classification of working areas. Given training samples  $\{(\mathbf{x}_i, z_i)\}$ ,  $\mathbf{x} \in \mathbb{R}^m$ ,  $z_i \in \{-1, 1\}$ ,  $i = 1, \dots, N$ , the two-class soft SVM is to find the Lagrange multipliers  $\xi = \{\xi_i\}_{i=1}^N$  such that [6]

$$J(\xi) = \sum_{i=1}^N \xi_i - \frac{1}{2} \sum_{i=1}^N \sum_{j=1}^N \xi_i \xi_j z_i z_j \phi(\mathbf{x}_i, \mathbf{x}_j) \quad (4)$$

is maximized subject to  $\sum_{i=1}^N \xi_i z_i = 0$  and  $0 \leq \xi_i \leq C$ .

Here  $C$  is the control parameter,  $\phi(\mathbf{x}_i, \mathbf{x}_j)$  is the kernel, and we take the linear kernel  $\phi(\mathbf{x}_i, \mathbf{x}_j) = \mathbf{x}_i^T \mathbf{x}_j$  for simplicity. Let  $\hat{\xi} = \{\hat{\xi}_i\}_{i=1}^N$  and  $b = b(\hat{\xi})$  be the optimal parameters such that  $f(\mathbf{x}) = 0$  will be the class boundary with  $f(\mathbf{x}) = \sum_{i=1}^N \hat{\xi}_i z_i k(\mathbf{x}, \mathbf{x}_i) - b$ .

In our case, we have three classes: clumped, good, and sparse working areas, denoted as C, G, and S, respectively. We employ the one-against-others method to form three 2-class SVMs for each pair of features. The maximum voting of the three is used to find the final classification results. During the training phase, the models of the three 2-class SVMs are learned from training data. In the test phase, each test sample  $\mathbf{x}$  has three predictions of class and the one having the largest prediction is the final decision.

### 4. Experiments and results

Our images are taken from malaria-infected Giemsa-stained blood smears using an oil immersion 100x objective. Their dimensions are  $M = 1024$  and  $N = 1280$  (pixels). So we have  $K = 9$ . We use sensitivity (SE), specificity (SP) and positive predictive value (PPV) to measure the performance of our method. SE measures the portion of images from true good working areas which are correctly classified. SP measures the portion of images from non-good working areas which are classified negatively. PPV is the portion of images classified as good areas and actually from good areas. We use 20 images for each class from one smear for training. Testing images are separate: 41 for "C", 48 for "G", and 45 for "S" from 2 other smears. All images are labeled by experts.

Fig. 4 shows scatter plots between features pairs of the test data where we can see the clusters of "G" and "C" are mixed up and are not easy to classify. The results of 15 classification methods are presented in Table I using 15 combinations of features, where columns correspond to performance measures of the methods and rows are the percentages of the same measure. Method 1 uses only occupancy to capture cell distribution. It has a low sensitivity but a high specificity and a positive predictive value. Method 2 uses feature  $\eta$  to give a high SE (100%) but both SP (45.35%) and PPV (50.53%) are rather low. It means

that it does not effectively identify the true GWAs.

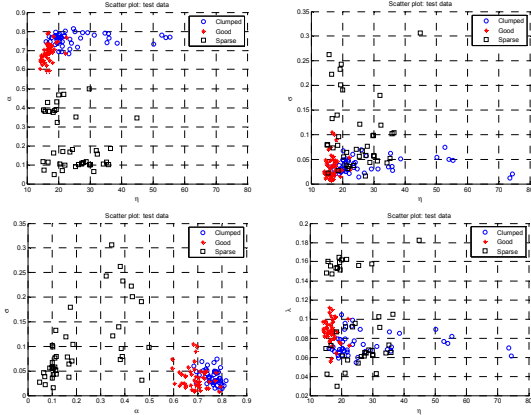


**Fig. 4. Scatter plots of pairs of features using the test data.**

**Table 1. Performance measures (%)**

Method	1, $\alpha$	2, $\eta$	3, $\sigma$	4, $\lambda$	5, $\tau$
SE	41.67	100.0	0.0	29.17	43.75
SP	95.35	45.35	100.0	86.05	70.93
PPV	83.33	50.53	0.0	53.85	45.65
Method	6, $\alpha, \eta$	7, $\alpha, \sigma$	8, $\alpha, \lambda$	9, $\alpha, \tau$	10, $\eta, \sigma$
SE	97.92	37.50	43.75	0.0	87.50
SP	76.74	95.34	97.67	100.0	68.60
PPV	70.15	81.82	91.30	0.0	60.87
Method	11, $\eta, \lambda$	12, $\eta, \tau$	13, $\alpha, \eta, \sigma$	14, $\alpha, \eta, \lambda$	15, $\alpha, \eta, \tau$
SE	95.83	100.0	97.92	97.92	97.92
SP	59.30	44.19	73.3	76.74	79.07
PPV	56.79	50.00	67.14	70.15	72.31

Features  $\alpha = \mu_0$  and  $\eta$  characterize the two different aspects of GWA and compensate for each other. Method 6 combines both features and produces much better results (SE= 97.92%, SP=76.74%, PPV= 70.15%). Method 3 uses the simple variance feature  $\sigma = \sigma_1$  at level 1. It has 100% specificity but zero sensitivity and positive prediction ability. Methods 4 and 5, which employ homogeneity features across scales, increase the two abilities greatly with good specificities. Usually, by utilizing clumping feature  $\eta$ , one can produce better sensitivities whereas by including homogeneity features, SE and PPV will be better. Both Methods 14 and 15 use the homogeneity features across scales defined here to achieve two best results. Finally, combining four features,  $(\alpha, \eta, \lambda, \sigma)$  and  $(\alpha, \eta, \lambda, \tau)$ , also produce good results (not shown in

Table I): SE=97.92%, SP=68.60%, PPV= 63.51%, and SE=97.92%, SP=79.07%, PPV=71.21%, respectively.

We use Matlab 7.4 calling SVM<sup>Torch</sup> [9] compiled in C++ with the linear kernel and  $C = 100$ . It takes a few seconds for feature extraction for each image and about 2 seconds for each classification method including both training and testing.

## 5. Discussion and conclusion

We have studied automatic classification of working areas in peripheral blood smears using generic features. There are 15 methods (including some using old techniques) compared. Basically, existing work is insufficient to characterize the GWA distribution thoroughly; adding crossing-scale features  $\lambda$  and  $\tau$  improves overall classification performance. It might be because both features encode the spatial distribution explicitly. However, we also encounter two strange results using these SE-SP-PPV indicators. Methods 3 and 9 produce the same performance numbers, as well as 6 and 14. For the former case, their confusion matrixes are different. Hence it seems that the matrixes convey more information. For the later, they have the same confusion matrixes. We will further study the topic in more detail and with more data.

## References

- [1] <http://www.niehs.nih.gov/research/atniehs/labs/lep/>.
- [2] J. V. Dacie and S. M. Lewis, *Practical Haematology*, Churchill Ltd., London, 1963.
- [3] L. Benattar and G. Flandrin, Comparison of classical manual pushed wedge films, with an improved automated method for making blood smears. *Hematology and cell Therapy*, 41: 1-5, 1999.
- [4] Jesus Angulo and G. Flandrin, Automated detection of working area of peripheral blood smears using mathematical morphology. *Analytical cellular pathology*, 25: 37-49, 2003.
- [5] Carl E. Mutschler, and Mark E. Warner, Pattern recognition system with working area detection. U.S. Patent 4702595. 1987.
- [6] John C. Russ, *The image Processing Handbook*, Second Edition, CRC Press, Inc, 1995.
- [7] L. Ballerini, A simple method to measure homogeneity of fat distribution in meat. *Proc. 12<sup>th</sup> Scandinavian Conference on Image Analysis*, Bergen, Norway, 2001.
- [8] N. Otsu, A Threshold Selection Method from Gray-Level Histograms. *IEEE Transactions on Systems, Man, and Cybernetics*, 9(1):62-66, 1979.
- [9] Ronan Collobert and Samy Bengio. SVM<sup>Torch</sup>: support vector machines for large-scale regression problems". *Journal of Machine Learning Research*, 1:143-160, 2001.